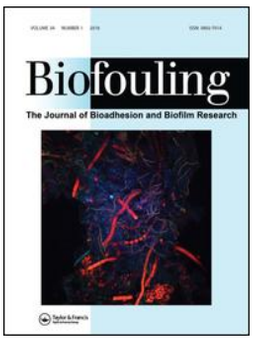

Taylor & Francis
Taylor & Francis Group

Biofouling
The Journal of Bioadhesion and Biofilm Research

ISSN: 0892-7014 (Print) 1029-2454 (Online) Journal homepage: https://www.tandfonline.com/loi/gbif20

Conditioning film formation and its influence on the initial adhesion and biofilm formation by a cyanobacterium on photobioreactor materials

Suvarna N. L. Talluri, Robb M. Winter & David R. Salem

To cite this article: Suvarna N. L. Talluri, Robb M. Winter & David R. Salem (2020): Conditioning film formation and its influence on the initial adhesion and biofilm formation by a cyanobacterium on photobioreactor materials, Biofouling

To link to this article: https://doi.org/10.1080/08927014.2020.1748186

Published online: 13 Apr 2020.

BIOFOULING
https://doi.org/10.1080/08927014.2020.1748186

Conditioning film formation and its influence on the initial adhesion and biofilm formation by a cyanobacterium on photobioreactor materials

Suvarna N. L. Talluri[a], Robb M. Winter[a] and David R. Salem[a,b,c]

[a]Department of Chemical and Biological Engineering, South Dakota School of Mines and Technology, Rapid City, SD, USA; [b]Composites and Polymer Engineering Laboratory, South Dakota School of Mines and Technology, Rapid City, SD, USA; [c]Composite and Nanocomposite Advanced Manufacturing - Biomaterials Center (CNAM-Bio), South Dakota School of Mines and Technology, Rapid City, SD, USA

ABSTRACT

Although cyanobacteria are a common group of microorganisms well-suited to utilization in photobioreactors (PBRs), studies of cyanobacteria fouling and its prevention are scarce. Using a cyanobacterium, *Anabaena* sp. PCC 7120, which had been genetically modified to enhance linalool production, the formation of conditioning films and the effects of these on the physicochemical surface properties of various PBR materials during initial adhesion and biofilm formation were investigated. The adhesion assay revealed that the overall attachment of *Anabaena* was substratum dependent and no correlation between the hydrophobicity/roughness of clean material and cell attachment was found. Surface hydrophilicity/hydrophobicity of all the materials changed within 12 h due to formation of conditioning films. ATR-FTIR spectroscopy revealed that the fractional change in protein deposition between 12 to 96 h was consistent with *Anabaena* cell attachment but polysaccharide deposition was material specific and did not correlate with cell attachment on the PBR materials. Also, the delay in conditioning film proteins on PVC and PTFE indicated that components other than proteins may be responsible for the decrease in contact angles on these surfaces within 12 h. This indicates the important role of the chemical nature of adsorbed conditioning films in determining the initial attachment of *Anabaena* to PBR materials. The lower rate of attachment of *Anabaena* on the hydrophilic surfaces (glass and PMMA) between 72 h to 96 h (regime 3) showed that these surfaces could potentially have low fouling characteristics at extended time scales and should be considered for further research.

ARTICLE HISTORY
Received 14 July 2019
Accepted 21 March 2020

KEYWORDS
Biofouling; photobioreactor; biofilm; conditioning film; adhesion mechanism; cyanobacteria

Introduction

About 80% of the world's energy is derived from fossil fuels which are non-renewable and finite (Caspeta et al. 2013). Fossil fuel burning releases carbon dioxide in high levels which is a major cause of global warming (Caspeta et al. 2013). The importance of replacing fossil fuels with renewable energy resources (such as biomass) to produce biofuels, and to decrease CO_2 levels in the atmosphere, is well recognized (Brennan and Owende 2010; Quintana et al. 2011; Caspeta et al. 2013). Third generation biofuels derived from cyanobacteria (blue-green algae) are gaining considerable importance (Parmar et al. 2011) due to their ability to capture CO_2 and sunlight to synthesize biofuels by photosynthesis (Callow and Callow 2002; Ducat et al. 2011). In general, cyanobacteria are cultivated in open ponds or closed photobioreactors (PBRs) for biofuel production (Rawat et al. 2013). Cyanobacteria cultivation in PBRs has several advantages over open ponds, including less risk of contamination, control over the process, and higher cell densities and productivities (Rawat et al. 2013). Despite their advantages, PBRs must overcome a number of challenges during their operation such as CO_2 depletion, oxygen accumulation along the tubes (Dragone et al. 2010) and poor light distribution due to fouling (Brennan and Owende 2010), all of which can negatively affect the biofuel productivity (Harris et al. 2013). In photobioreactors, light distribution plays an important role in cyanobacterial photosynthesis (Wang et al. 2012). Fouling on light transmitting surfaces can cause poor utilization of light energy by cyanobacteria which can ultimately decrease the biomass generation and biofuel productivity (Harris et al. 2013). Fouling can also result in frequent shut down of photobioreactors for cleaning which can be a

CONTACT David R. Salem David.Salem@sdsmt.edu; Robb M. Winter Robb.Winter@sdsmt.edu

major problem in continuous production of biofuels (Tsoglin et al. 1996; O'Connor 2011, 9). Many antifouling (AF) technologies have been developed with a focus on preventing medical, industrial and marine biofouling by different microorganisms over the years (Bixler and Bhushan 2012; Damodaran and Murthy 2016; Nir and Reches 2016). Very few studies have discussed the applicability of those technologies to photobioreactors (Wang et al. 2017; Zeriouh et al. 2017; 2019). A study conducted by Wang et al. (2017) used chemical modification of polyethylene (PE), a commonly used photobioreactor material, to develop AF PE films surface-grafted with sulfobetaine polymers due to their hydrophilic nature that resist microalgal colonization (Wang et al. 2017). Another study by Zeriouh et al. (2017) suggested using foul release (FR) materials such as fluoropolymers and silicone-based polymers for manufacturing PBRs, mainly because of their low surface energy and ultra-smooth characteristics which can prevent organisms from settling on the surfaces (Zeriouh et al. 2017). A study by Zeriouh et al. (2019) used polycarbonate coated with a commercial silicone-hydrogel based FR coating to prevent the attachment of a microalga (N. *gaditana*) and found that these coatings exhibited promising AF properties without affecting the growth and viability of the microalgal cells (Zeriouh et al. 2019). Even though all these materials showed AF properties, so far none was tested against cyanobacterial biofilms. Many authors have reported fouling as a limiting factor for biofuel production in PBRs (Brennan and Owende 2010; Dasgupta et al. 2010; Dragone et al. 2010) but studies that describe the strategies to overcome cyanobacterial fouling in PBRs are scarce. This is mainly because cyanobacterial species are not as well explored as other bacteria (Irving and Allen 2011; Sirmerova et al. 2013) and eukaryotic microalgae (Zeriouh et al. 2017; 2019) in relation to fouling, and currently known mechanisms of cyanobacteria adhesion have been insufficient to prevent the formation of cyanobacteria biofilms on PBRs (Schatz et al. 2013). Therefore, it is important to understand the factors influencing adhesion of cyanobacteria to PBR materials in any effort to identify biofouling mechanisms.

Biofouling is a well-known phenomenon which occurs when microorganisms switch from a free-living planktonic state to surface attached sessile communities called biofilms (Kolter and Greenberg 2006). In most cases, biological material called a conditioning film adsorbed on to the submerged surface initiates the process of biofilm formation (Gademann 2007). Conditioning film formation on a solid surface is reported to influence initial bacterial adhesion by altering substratum properties such as surface roughness, surface charge, chemical composition and surface hydrophobicity/hydrophilicity (Gubner and Beech 2000; Lorite et al. 2011; Hwang et al. 2012). The second step of the process is the reversible adhesion of microorganisms to the conditioning film. In this process bacteria can use extracellular organelles such as flagella and pili to sense and attach to the conditioning film (Renner and Weibel 2011). In the third step, microorganisms are irreversibly adhered to the conditioning film by secreting extracellular polymeric substances (EPS) (Hoiczyk 2000).

A number of reports indicate that surfaces with high roughness and hydrophobic properties are favorable for cyanobacterial adhesion (Callow et al. 2000; Sekar et al. 2004; Ozkan and Berberoglu 2013), but there are also studies which show no correlation between the hydrophobicity and roughness of the surfaces and cell attachment (Katsikogianni and Missirlis 2004; Irving and Allen 2011). These contradictory results arise mainly because, even though surface roughness and hydrophobicity are considered to be fundamental properties for cell attachment, these substratum surface properties can be readily masked by the formation of conditioning films (Whitehead and Verran 2009; Lorite et al. 2011). Studies have reported that, more than the surface hydrophobicity and roughness, surface chemical functional groups resulting from the conditioning films have an important role in bacterial adhesion to substrata (Gubner and Beech 2000; Lorite et al. 2011). Despite their importance in early stage biofilm formation, the formation of conditioning films is not a well understood process (Siboni et al. 2007). This is mainly because the composition of conditioning films vary, depending on the kind of microorganisms involved, the growth medium in which the material is suspended, and the nature of the material (Compere et al. 2001; Donlan 2002). Therefore, the dynamics of conditioning film formation and their influence on early stage biofilm development need to be explored in order to understand the mechanisms related to cyanobacterial adhesion on PBR materials (Siboni et al. 2007).

Several species of cyanobacterial genera have been extensively studied due to their capability to utilize CO_2, sunlight and wastewater to produce oxygen and biofuels (Mostafa et al. 2012). *Anabaena* sp. PCC 7120, a filamentous nitrogen fixing cyanobacterium, was found to be an excellent host for the production

of high value chemicals, as well as for removing heavy metals from industrial wastewater (Ruffing 2011). Considering the ability of this organism to survive in high levels of CO_2 (Thomas et al. 2005) and to treat wastewater (Ruffing 2011), a National Aeronautics and Space Administration (NASA) program was undertaken to develop a PBR system for cultivation of *Anabaena* sp. PCC 7120 (Duke 2011) which had been genetically engineered to produce oxygen and linalool (a platform chemical) directly from CO_2 and sunlight (Duke 2011; Zhou and Gibbons 2015). The long-term goal of this PBR system is to provide life support conditions for space colonizing missions by producing oxygen and fuels in a sustainable manner by converting CO_2 and wastewater (Duke 2011).

Therefore, in this study, *Anabaena* sp. PCC 7120, genetically engineered to produce linalool (engineered *Anabaena*), was used as a model organism to study biofouling on PBR materials. Details of linalool production from this *Anabaena* can be found in a patent by Zhou and Gibbons (2015). Widely used PBR materials that satisfy the transparency requirement for PBR construction include glass, polyvinyl chloride (PVC), poly(methyl methacrylate) (PMMA), polycarbonate (PC) and high-density polyethylene (HDPE) (Wang et al. 2012; Genin et al. 2014). In the present study, these materials were taken as model surfaces/substrata, together with polytetrafluoroethylene (PTFE), a non-transparent substratum selected for its low surface energy rather than for its suitability as a PBR material. The main objective of this study was to investigate the role of conditioning films and their influence on initial adhesion and biofilm formation of the engineered *Anabaena* to PBR materials. This was done by evaluating the physico-chemical changes occurring on PBR materials, starting from the evolution of conditioning film formation to biofilm development by the engineered *Anabaena* cells, on a time scale of up to 96 h.

Materials and methods

Substratum materials and preparation

Suitable photobioreactor materials, *viz.* glass, poly (methyl methacrylate) (PMMA), poly vinyl chloride (PVC), polycarbonate (PC) and high-density polyethylene (HDPE) were selected as substratum materials. Polytetrafluoroethylene (PTFE), a material that possesses low surface energy and a low degree of biofouling retention characteristics (Yebra et al. 2004; Kirschner and Brennan 2012), was used for comparison with the PBR materials. Soda lime glass microscope slides ($25 \times 75 \times 1$ mm) were purchased from Fisher Scientific (Pittsburgh, PA, USA) and polymer sheets (thickness of 1 mm) were purchased from Goodfellow Corporation (Coraopolis, PA, USA). All the substratum materials were cut into coupons of dimensions 50×15 mm. The polymer coupons were cleaned by rinsing in 70% ethanol followed by vigorous rinsing in deionized water (Cui et al. 2013). Glass coupons were cleaned by sonicating for 10 min in 1 N HCl followed by rinsing in deionized water, 70% ethanol and again with deionized water (Hwang et al. 2012). The cleaned substratum materials were air dried under aseptic conditions and characterized by various experimental methods such as contact angle goniometry, attenuated total reflectance–Fourier transform infrared (ATR-FTIR) spectroscopy and atomic force microscopy (AFM). Finally, all the cleaned materials prepared were stored in sterile deionized water until they were used for experiments.

Cyanobacterium and culture conditions

A pure culture of *Anabaena* sp. PCC 7120, genetically engineered to produce linalool, was taken as a model organism. Linalool-producing, genetically engineered *Anabaena* sp. PCC 7120 (engineered *Anabaena*) was provided by Drs R. Zhou and W. Gibbons of the Biology and Microbiology department at South Dakota State University, Brookings, SD (Zhou and Gibbons 2015). The engineered *Anabaena* strain was cultivated in modified BG-11 medium containing 100 μg ml^{-1} of neomycin (Rippka et al. 1979; Zhou and Gibbons 2015). The modified BG-11 medium was prepared by adding 1.5 g of $NaNO_3$, 0.0366 g of $MgSO_4 \bullet 7H_2O$, 0.036 g of $CaCl_2 \bullet 2H_2O$, 0.04 g of $K_2HPO_4 \bullet 3H_2O$, 0.006 g of citric acid, 0.006 g of ferric ammonium citrate, 0.001 g of EDTA (disodium magnesium salt), 0.02 g of Na_2CO_3 and 1 ml of trace element mix A5 + Co in 1 l of deionized (DI) water. Trace element mix A5 + Co solution was prepared by adding the following components to 1 l of DI water: 2.86 g of H_3BO_3, 1.81 g of $MnCl_2 \bullet H_2O$, 0.222 g of $ZnSO_4 \bullet 7H_2O$, 0.39 g of $Na_2MoO_4 \bullet 2H_2O$, 0.079 g of $CuSO_4 \bullet 5H_2O$, and 0.0494 g of Co $(NO_3)_2 \bullet 6H_2O$. The initial pH of the prepared BG-11 medium was set at 7.1. Unless specified otherwise, the engineered *Anabaena* was grown in 500 ml Erlenmeyer flasks containing 200 ml of sterile BG-11 medium with 100 μg ml^{-1} of neomycin. The flasks were continuously shaken at 150 rpm in an orbital incubator shaker at 30 °C under a light intensity of 25-30 micro-einsteins m^{-2} s^{-1} (Rippka et al. 1979; Zhou and

Gibbons 2015). Throughout the study, the engineered *Anabaena* was grown under atmospheric air until the culture reached the exponential phase (optical density 0.7–0.8).

Initial adhesion of engineered Anabaena to substrata

An initial adhesion assay of engineered *Anabaena* on substratum materials was conducted by a modified method described by Irving and Allen (2011). Agar plates were prepared by adding 30 ml of sterile agar (1% agar made in modified BG-11 medium containing 100 µg ml^{-1} of neomycin) medium to large (100 mm diameter) Petri dishes. Agar in the Petri dish was cut with a sterile scalpel blade in such a way that the coupons of 50 × 15 mm could be inserted. In this way several replicate Petri dishes were made by inserting the coupons, and 30 ml of engineered *Anabaena* cell suspension (8×10^7 cells ml^{-1}) containing 100 µg ml^{-1} neomycin was poured into the Petri dishes. The Petri dishes were incubated at 30 °C under a light intensity of 25-30 microeinsteins m^{-2} s^{-1}. The same procedure was applied to all the substratum materials. Six replicate coupons were collected at each time interval for all the substratum materials up to 96 h during the course of adhesion of the engineered *Anabaena* cells (Sekar et al. 2004; Irving and Allen 2011). The coupons were gently rinsed in deionized water to remove loosely bound cells, air dried at room temperature overnight (Sekar et al. 2004) and characterized by different analytical techniques described in the following section. Among the six replicate coupons collected at each time interval, three were used for microscopic imaging and contact angle measurements and the other three were used for ATR-FTIR spectroscopy and atomic force microscope analyses.

Analytical methods

Bright field microscopy

The initial adhesion of engineered *Anabaena* cells on different substratum materials was observed by reflected-light bright field microscopy using an upright microscope (Carl Zeiss Axio Imager.M1m, Thornwood, NY, USA). Twenty images from each of the three replicate coupons were captured in random fields using AxioVision LE software. The images were processed in ImageJ (Rasband 1997) to calculate the percentage area occupied by the engineered *Anabaena* cells on the different materials (Rasband 1997; Chung et al. 2007). Briefly, the image background was adjusted using Process-Subtract Background command. The brightness of the image was adjusted using Image- Adjust-Brightness/Contrast command to highlight the cells and lighten the surrounding deposited material. Image-Adjust-Threshold command was used to enhance the area occupied by cells. Using Analyze-Analyze Particles command, the percentage area occupied by cells was calculated (Rasband 1997; Chung et al. 2007). The mean percentage area coverage of engineered *Anabaena* was calculated based on the independent means from three replicate coupons for all the materials at each time interval.

Contact angle measurements

The water contact angles of the clean and biofilm-adhered materials were measured by the sessile drop method using a contact angle goniometer (Model 500, Rame-hart Instrument Co., Succasunna, NJ, USA) (Thome et al. 2014). Six drops were placed on each of the three replicate coupons and contact angles were averaged. In the case of polymer materials, 5 µl water drops were placed whereas in the case of glass, 2 µl water drops were placed to properly visualize the left and right angles of the droplets in DROP image software.

ATR-FTIR spectroscopy

An Agilent Cary 660 FTIR spectrometer equipped with diamond ATR (Agilent Technologies, Santa Clara, CA) was used to obtain the infrared spectra of clean and biofilm adhered substratum materials. The diamond crystal was cleaned with acetone before each measurement. Coupons were pressed against the diamond crystal using a pressure clamp ensuring that the biofilms attached to the substrata were in close contact with the crystal. Spectra were collected at a spectral resolution of 4 cm^{-1} and averaged over 100 scans within the wavenumber region of 1800 cm^{-1} and 800 cm^{-1} (Lorite et al. 2011). Spectra from at least two separate locations of each of the three replicate coupons (total of six spectra for each time interval for all the materials) were collected and processed in Agilent Resolutions Pro software version 5.2.0. All the sample spectra were baseline corrected, averaged and subtracted from the spectra of respective clean substrata (Resolutions Pro software, Version 5.2.0. Agilent). An optimum subtraction factor that minimizes the absorbance/intensity of a number of interfering substratum polymer/glass peaks in the wavenumber region 1750 to 950 cm^{-1} was chosen (Smith 2011, 59–60) to produce the difference spectra

(Kunov-Kruse et al. 2013) of all the materials at each time interval. Each spectrum was normalized to the absorbance of the peak that had a maximum absorbance within the spectrum for a direct comparison between the different time intervals (Smith 2011, 79–80) and deconvoluted using Peakfit 4.12 software (Systat software Inc., San Jose, California, USA) (Kunov-Kruse et al. 2013). The built-in Voigt area algorithm was used for peak fitting and the integrated areas of the peaks obtained from deconvolution were used to assess and quantify the contribution of specific surface chemical functional groups (Parikh and Chorover 2006; Kunov-Kruse et al. 2013). Deconvolution was carried out until the model converged the experimental data to R^2 values between 0.99 – 1.00.

Atomic force microscopy (AFM)

Surface topography images of the clean substratum materials were captured by a multimode atomic force microscope (Multimode 8, Bruker, Santa Barbara, CA, USA). The multimode 8 atomic force microscope was operated in tapping mode using a silicon probe with a spring constant of 3 N m^{-1}, a radius of 8 nm, a height of 15-20 µm and a resonance frequency of 75 KHz, purchased from Bruker AFM probes (Bruker AFM probes, Camarillo, CA, USA). Topography images were obtained with a scan area of 10 × 10 µm. Images of at least five random locations from each of the three replicate coupons were captured for all the materials. All the images were processed in Nanoscope 8.15 software using Flatten and Clean Image commands prior to the analysis (Auerbach et al. 2000). Flatten command was used to eliminate the noise, bow and tilt of the images and Clean Image command was used to smooth the noisy image. The root mean square roughness (Rq) of the clean substratum materials was calculated using the roughness analysis function (Auerbach et al. 2000; Lorite et al. 2011).

Statistical analysis

The statistical differences in the mean percentage area coverage of *Anabaena* between different substratum materials across different time points (24 h, 48 h, 72 h and 96 h) were evaluated by mixed analysis of variance (mixed ANOVA) with one "between-subjects" factor (material) and one "within-subjects" factor (time) followed by Tukey's *post hoc* test for multiple comparisons of means with Bonferroni correction. Three replicate coupons were nested within each material for all time points. Mixed ANOVA (replicates were nested within material) was carried out to evaluate the statistical differences in the mean contact angles between the substratum materials at 0 h, 12 h, 24 h, 48 h, 72 h and 96 h followed by Tukey's *post hoc* test for multiple comparisons of means with Bonferroni correction. The univariate analysis of variance (Univariate ANOVA) was conducted on contact angles (and surface roughness) of clean materials as a dependent variable and material as an independent variable followed by Tukey's HSD *post hoc* test for multiple comparisons of means with Bonferroni correction. Three replicate coupons were nested within each material for analysis and statistical differences in mean contact angles and surface roughness between different clean substrate materials were evaluated. Statistical analyses were conducted using SPSS v27.0 statistical software.

Table 1. Water contact angle, root-mean-squared (R_q) roughness of clean substratum materials.

Material	Water contact angle ± SD (°)	Surface roughness ± SD (R_q) (nm)
Glass	16.9 ± 1.4	1.2 ± 0.1
PMMA	85.4 ± 1.1	3.5 ± 0.8
PVC	86.7 ± 3.3	4.2 ± 0.5
PC	92.8 ± 1.0	3.9 ± 1.2
HDPE	91.4 ± 2.3	21.7 ± 4.1
PTFE	110.3 ± 1.6	85.0 ± 19.2

Values represent the means ± the SD of the three-independent means ($n = 3$).

Results and discussion

Characterization of clean substrata

Clean substratum materials were characterized by three methods. The hydrophobicity/hydrophilicity of the materials were determined by contact angle measurements (Table 1), which were in close agreement with the values reported in the literature (Husmark and Rönner 1993; Hwang et al. 2012). Univariate analysis of variance showed significant differences in the mean contact angles of the different substratum materials, $F(5,90) = 2876.14$, $p < .001$. Having contact angles of < 90°, the glass, PMMA and PVC surfaces were found to be hydrophilic. The PC, HDPE and PTFE surfaces were found to be hydrophobic, having contact angles > 90° (Table 1). Tukey's *post hoc* test revealed that there were significant differences in the contact angles between all the materials (Tukey's test, $p < .05$) except for hydrophilic PMMA and PVC and hydrophobic PC and HDPE (Table 1). The surface chemistry of the materials was examined by ATR-FTIR spectroscopy and was consistent with the expected chemical compositions of the materials

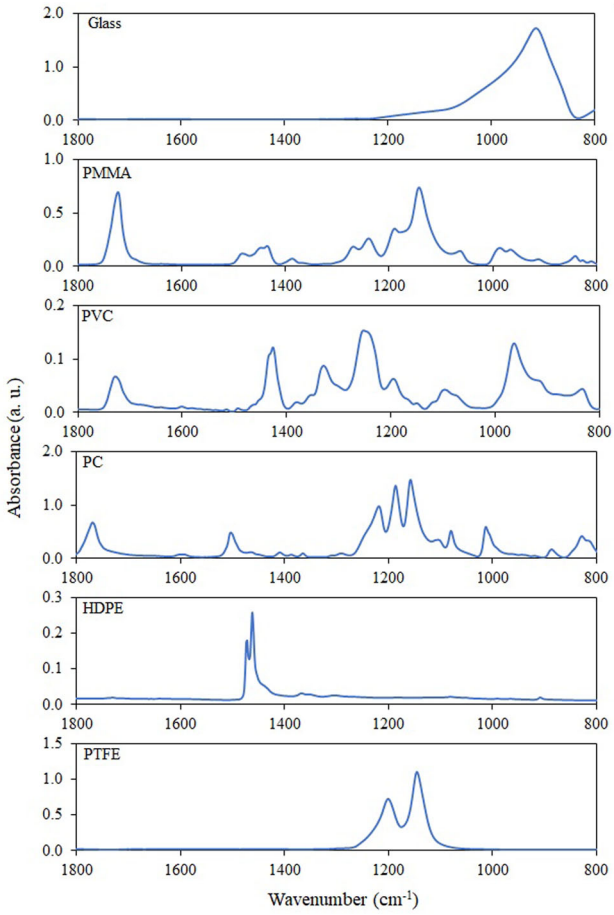

Figure 1. ATR-FTIR spectra of clean substratum materials.

(Figure 1). The surface topography of the materials captured by atomic force microscopy, the section analysis conducted on the topography images and the respective line profiles are shown in Figure 2. The line profiles indicate the height differences across the section created on the topography images of the different materials. The root-mean-squared roughness (R_q) of the materials are reported in Table 1. Univariate analysis of variance revealed significant differences in average surface roughness of the different substratum materials, $F(5,72) = 1186.91$, $p < .001$. Surface roughness measurements revealed that, on the nanoscale, the HDPE (R_q of ~22 nm) and PTFE (R_q of ~85 nm) samples had rough surfaces compared with glass, PMMA, PVC and PC (R_q < 5 nm) (Tukey's test, $p < .05$ for each combination) (Table 1 and Figure 2).

Initial adhesion of engineered Anabaena to substratum materials

The initial adhesion of engineered *Anabaena* cells on different substratum materials was observed by bright field microscopy (Figure 3) and quantified by measuring the percentage area coverage of engineered *Anabaena* using ImageJ (Figure 4). Figure 4 shows the changes in the percentage area coverage of engineered *Anabaena* on the different materials with time. A mixed ANOVA was conducted to assess whether there were any statistically significant changes in the percentage area coverage between the materials across different time intervals during the adhesion of *Anabaena* (Figure 4). The results indicate that there were statistically significant differences in the overall coverage of *Anabaena* between the different materials $F(5,342) = 156.80$, $p < .001$ and across the four-time intervals $F(1.304,446.04) = 1468.91$, $p < .001$ examined. There was also a significant interaction between the time and material $F(6.521,446.04) = 163.18$, $p < .001$. At 96 h, the total area occupied by engineered *Anabaena* cells was higher on PTFE (~5.4%) and PC (~3.6%), compared with HDPE (~1.6%), glass (~1.5%), PMMA (~1.2%) and PVC (~1.0%) (Tukey's test, $p < .05$ for each combination). Interestingly, the initial colonization of *Anabaena* was delayed on PC and PTFE (~72 h) compared with the relatively rapid colonization of glass (~24 h), PMMA (~48 h) and HDPE (~48 h), despite the lower overall coverage of cells on glass, PMMA and HDPE than on PC and PTFE at 96 h (Tukey's test, $p < .05$ for each combination). Even though there were no significant changes in *Anabaena* attachment on PVC, PMMA and glass surfaces (Figure 4) at 96 h (Tukey's test, $p > .05$ for each combination), initial colonization was not apparent on PVC until 72 h (Figure 3). Although the percentage area coverage of engineered *Anabaena* cells on the different materials varied (Figure 4), the early stage of first-layer biofilm formation was observed on all the materials at 96 h (Figure 3). From the representative images of the adhesion of engineered *Anabaena* cells on the different substratum materials over time (Figure 3) it can be seen that the engineered *Anabaena* was attached to all the substrata in the form of single cells or filaments. Figure 3 also gives an indication of deposits (gray material identified with red arrows) between the cells/filaments (shown in black) of the *Anabaena* on all the materials. These deposits, which were left on the surfaces when the loosely bound cells were washed away during rinsing, have been referred to as EPS by several authors (Azeredo and Oliveira 2003; Lorite et al. 2011). These EPS deposits could be a contribution from different forms of EPS such as capsulated polysaccharides (CPS) and/or released polysaccharides (RPS) (Richert et al. 2005) and/or biofilm polysaccharides (Beech et al. 1999) that *Anabaena* cells

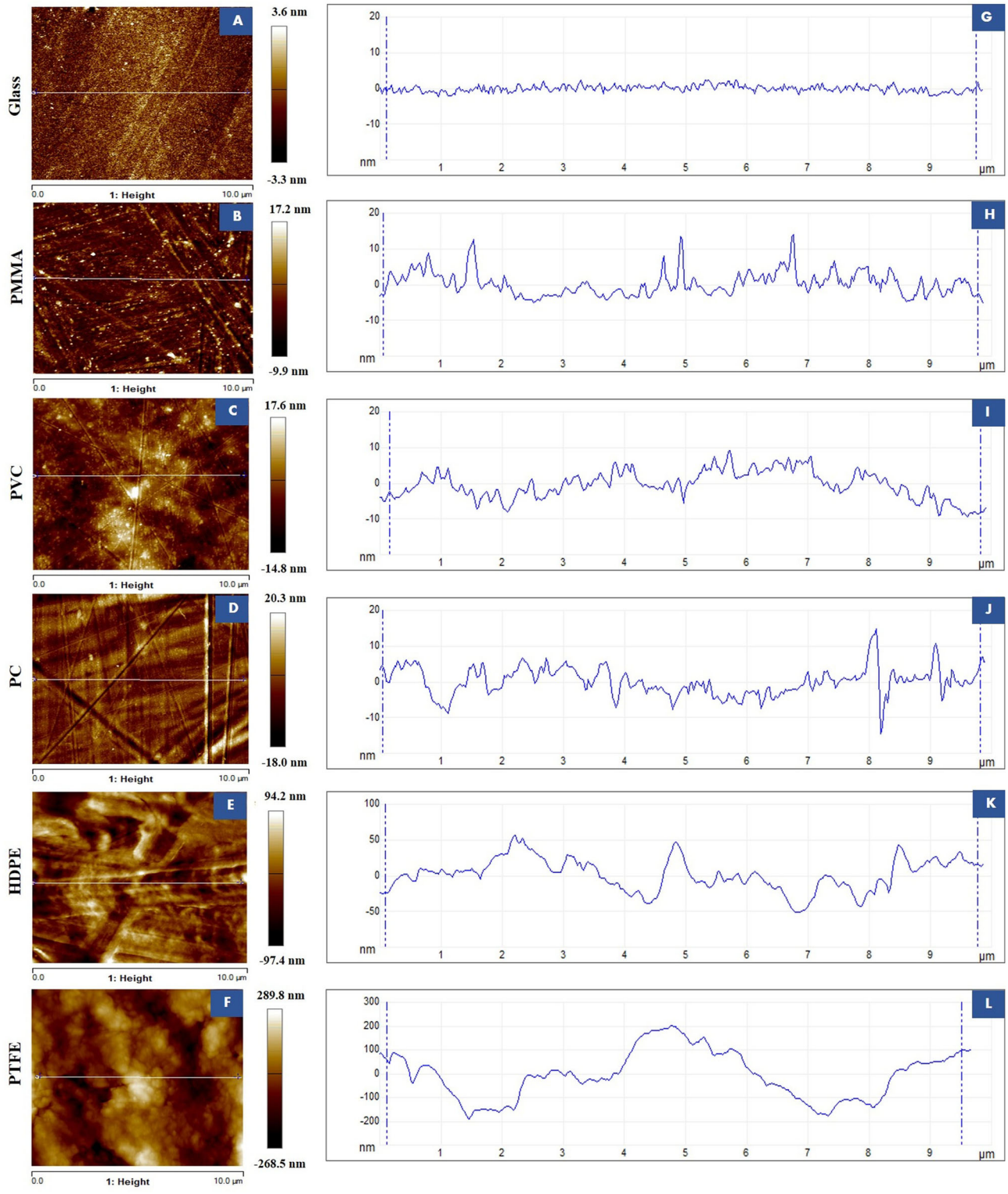

Figure 2. AFM topography (A to F) and line profiles obtained from section analysis of the topography images (G to L) of clean substratum materials.

produce during the phases of growth, adhesion and biofilm development. These EPS deposits may contain compounds secreted from the *Anabaena* such as polysaccharides, lipids, nucleic acids, proteins, inorganic and organic substituents, which may influence the adhesion of the *Anabaena* cells to substrata (De Philippis and Vincenzini 1998; De Philippis et al. 2001; Azeredo and Oliveira 2003).

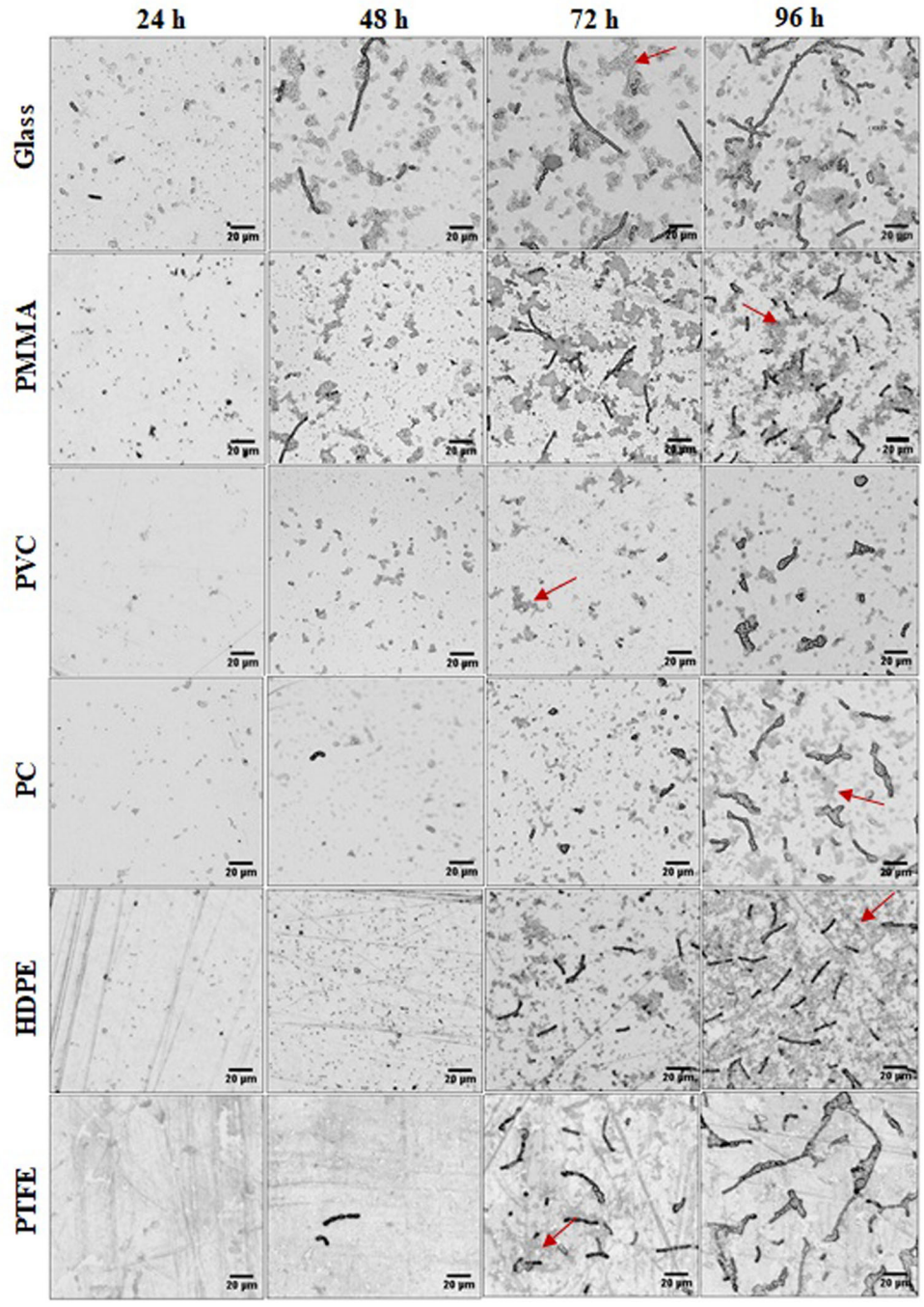

Figure 3. Representative bright field microscopy images of engineered *Anabaena* attached on different substratum materials over a period of 96 h (scale bars = 20 µm). The engineered *Anabaena* cells and filaments are shown in black and the grey material is the residue of EPS left on the surface when the loosely bound cells were removed by rinsing. The streaks observed, mostly on HDPE and PTFE, could be due to higher roughness and depressions on these surfaces as observed from AFM images of the clean substrata in Figure 2.

Studies have shown that the bacteria in general prefer to attach to hydrophobic and rough surfaces (Callow et al. 2000; Sekar et al. 2004; Lorite et al. 2011; Ozkan and Berberoglu 2013). In studies conducted by Callow et al. (2000) and Sekar et al. (2004), different cyanobacteria and green algal species were tested for their ability to attach to hydrophobic and hydrophilic materials and it was found that the cell density was higher on hydrophobic materials compared with hydrophilic surfaces. The authors explained that this differential attachment density of bacteria on hydrophobic and hydrophilic materials

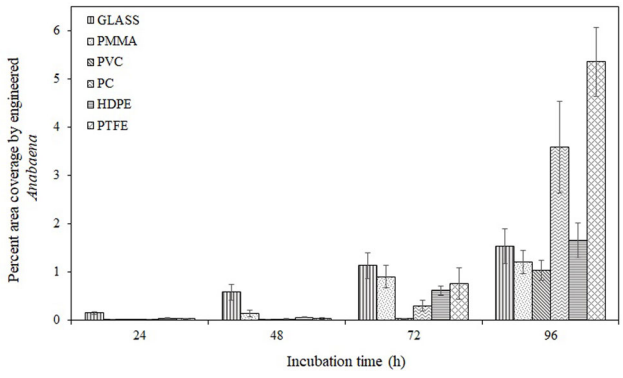

Figure 4. Initial adhesion of engineered *Anabaena* cells on different substratum materials with time. Error bars represent ± SEs ($n = 3$). The mean percent area coverage and standard error were calculated based on three independent means at each time interval for all the materials.

was mediated by a water exclusion mechanism (Sekar et al. 2004). According to this mechanism, easier displacement of water molecules from hydrophobic surfaces facilitates the adhesive bonding between cells and substratum resulting in a higher density of cells, whereas in the case of hydrophilic surfaces, cells were not able to form an adhesive bond which resulted in a lower density of cells on these surfaces (Callow et al. 2000). Hydrophilic substrata interact strongly with water molecules through hydrogen bonding so the displacement of surface bound water molecules from hydrophilic surfaces is a major barrier for adhesion of cells (Petrone 2013). In the present study, the overall lower attachment on hydrophilic glass, PMMA and PVC than on hydrophobic PC and PTFE (Figure 4) at 96 h (Tukey's test, $p < .05$ for each combination) could involve a similar mechanism. However, although HDPE was also a hydrophobic surface, the percentage area coverage of *Anabaena* was not much higher than on the hydrophilic surfaces of glass and PMMA (Figure 4) (Tukey's test, $p > .05$ for each combination), which indicates that *Anabaena* attachment on all the materials cannot be described solely by the water exclusion mechanism.

It is also possible that the overall higher attachment of engineered *Anabaena* cells on PTFE than on the other materials at 96 h (Figure 4) (Mixed ANOVA $p < .001$, Tukey's test, $p < .05$ for each combination) may be related to the higher roughness of this material ($R_q = \sim 85$ nm) than the other substrata (Table 1) (Univariate ANOVA $p < .001$, Tukey's test $p < .05$ for each combination). Increased surface area resulting from depressions and the overall higher roughness of the PTFE surface could have created favorable sites for colonization of the *Anabaena* cells (Katsikogianni and Missirlis 2004; Sekar et al. 2004). On the other hand, on HDPE, which is the second roughest material ($R_q \sim 22$ nm), the attachment of *Anabaena* was lower (Figure 4) than on PC ($R_q = \sim 4$ nm) (Mixed ANOVA $p < .001$, Tukey's test, $p < .05$) which indicates that the surface roughness of clean substrata alone cannot describe the different attachment behavior of the engineered *Anabaena* on these materials. Also, the statistically insignificant difference in the overall attachment of *Anabaena* on smooth hydrophilic glass and rough hydrophobic HDPE at 96 h (Figure 4 and Table 1) (Tukey's test, $p > .05$) suggests that factors other than clean material hydrophobicity and roughness may be involved (Cui et al. 2010; Lorite et al. 2011). As with other bacteria, attachment of cyanobacteria to substrata is facilitated by the production of EPS, and the variation in cell attachment could also be influenced by differences in the ability of the *Anabaena* to deposit EPS on the different surfaces (De Philippis and Vincenzini 1998; De Philippis et al. 2001; Sekar et al. 2004). Overall, a lack of correlation between the properties of the clean substratum (hydrophobicity and roughness) and *Anabaena* attachment in this study indicates the need for evaluation of the physico-chemical changes occurring on the materials due to conditioning film formation. Very few studies have focused on the occurrence of conditioning films on different substrata (Compere et al. 2001; Garg et al. 2009; Leefmann et al. 2015) and their role in adhesion of bacteria (Jain and Bhosle 2009; Lorite et al. 2011; Hwang et al. 2012, 2013) and green algae (Ladner et al. 2010; Thome et al. 2012), and currently reports do not exist on how the substratum properties may be altered by compounds secreted from cyanobacteria, and the conditioning films that are formed. Therefore, it is important to investigate the physico-chemical changes occurring on substratum materials during the initial adhesion of engineered *Anabaena* for deeper understanding of the molecular mechanisms involved.

Surface physico-chemical changes occurring during the initial adhesion of engineered Anabaena on substratum materials and the role of conditioning films

Changes in the physico-chemical properties, specifically the surface hydrophobicity/hydrophilicity and the surface chemistry of different materials during the initial adhesion of the engineered *Anabaena* were determined by contact angle measurements and ATR-FTIR spectroscopy. Figure 5 shows the time dependent changes in the contact angles of substrata during the

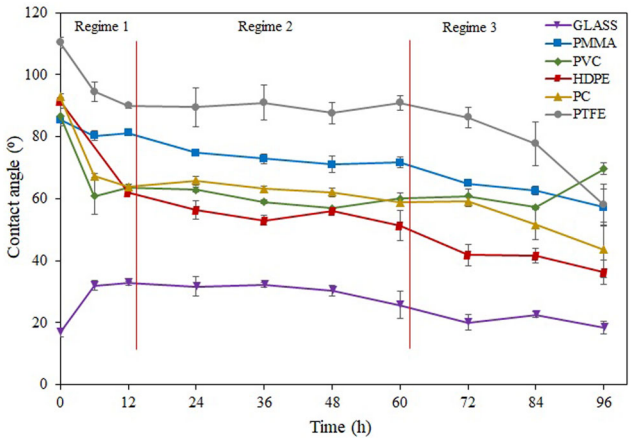

Figure 5. Change in contact angle of substratum materials with time during the initial adhesion of engineered *Anabaena* cells. Error bars represent the SD of the mean ($n = 3$).

initial adhesion of *Anabaena*. There was a change in contact angles of all the materials within 6–12 h of immersion of the substrata in the *Anabaena* suspension. A mixed ANOVA was conducted to evaluate the statistically significant differences in the average contact angles between the different substratum materials at different time points during the adhesion of *Anabaena* (Table 2). The results revealed that there were significant differences in the contact angles between the different materials $F(5,90) = 5819.48$, $p < .001$ and across the six-time intervals $F(5,450) = 1637.27$, $p < .001$ examined. A significant interaction effect was also observed between the time and material $F(25,450) = 189.41$, $p < .001$. The contact angles of all the polymer substrata decreased as the time changed from 0 to 96 h (Tukey's test, $p < .05$). Hydrophobic PC, HDPE and PTFE became hydrophilic within 12 h (Table 2) (Tukey's test, $p < .05$). Hydrophilic surfaces such as PMMA and PVC became more hydrophilic within 12 h (Table 2) (Tukey's test, $p < .05$). In contrast to this, the contact angle of hydrophilic glass increased slightly within 12 h (Table 2) (Tukey's test, $p < .05$). The change in contact angle of all the materials within a few hours of immersion of the substrata in this study was in good agreement with the literature on other microbes (Thome et al. 2012). These contact angle changes could be due to conditioning film formation (Thome et al. 2012) because there was no indication of *Anabaena* cell attachment on any of the substrata at 12 h (data not shown). Following this initial change (regime 1), the contact angle remained essentially constant for all the materials until about 60 h (regime 2) (Figure 5). At some point, in the range from about 60–96 h (regime 3), the contact angle decreased in all the materials except PVC, where it increased. The contact angle decrease was particularly strong for PTFE in this regime.

Table 2. Contact angle measurements of different substratum materials changing with time.

Time (h)	Contact angles ± SD (°)					
	Glass	PMMA	PVC	PC	HDPE	PTFE
0	16.9 ± 1.4	85.4 ± 1.1	86.7 ± 3.3	92.8 ± 1.0	91.4 ± 2.3	110.3 ± 1.6
12	32.6 ± 0.6	81.2 ± 0.9	63.7 ± 0.3	63.8 ± 1.0	62.1 ± 0.7	90.0 ± 0.9
24	31.7 ± 3.1	74.8 ± 1.2	62.8 ± 0.7	65.8 ± 1.4	56.3 ± 3.1	89.4 ± 6.4
48	30.4 ± 1.7	71.0 ± 2.7	56.8 ± 0.4	62.0 ± 1.4	56.0 ± 0.1	87.6 ± 3.3
72	20.0 ± 2.6	64.8 ± 0.3	60.8 ± 2.3	59.0 ± 1.7	41.8 ± 3.6	86.1 ± 3.3
96	18.3 ± 2.1	57.2 ± 6.0	69.6 ± 1.8	43.5 ± 8.9	36.3 ± 3.9	58.0 ± 6.5

Values represent the means ± the SDs of the three-independent means ($n = 3$).

Since Figures 3 and 4 indicate little cell growth in regime 2, with the exception of the glass substratum, this regime may be associated with further coverage of the surface by conditioning film and, possibly, reversible adhesion of the *Anabaena* cells. Regime 3, on the other hand, appears to be associated with strong cell growth (Figures 3 and 4) and may be associated with the irreversible attachment of the engineered *Anabaena* cells, involving the secretion of EPS (Beech et al. 2005; Siboni et al. 2007; Lorite et al. 2011). From the mechanism of biofouling, EPS production facilitates the irreversible adhesion of cells, but the EPS deposits left on the surface by the loosely bound cells (Figure 3) reveals that despite the presence of EPS, irreversible attachment of cells may be taking place only in certain areas on the surface. It is possible that the *Anabaena* cells might be producing chemically different EPS in different locations within the biofilm which may influence the extent of reversibility of the cells on the materials.

In order to obtain information about the chemical functional groups involved in the initial adhesion of the engineered *Anabaena*, ATR-FTIR spectroscopy was applied on materials incubated in *Anabaena* suspension for up to 96 h. The normalized difference spectra in Figure 6 show the time-dependent evolution of absorption peaks during *Anabaena* adhesion to glass, PMMA, PVC, HDPE, PC and PTFE in the wavenumber region 1750 to 950 cm^{-1} where chemical functional groups of important biomolecules such as proteins, polysaccharides, lipids and nucleic acids appear (Dean and Sigee 2006; Parikh and Chorover 2006). The bands near 1652 cm^{-1} and 1546 cm^{-1}, which represent the proteins, were cleanly subtracted. However, with the exception of HDPE, the interference of clean substratum polymer/glass peaks (Figure 1) was evident for all the materials in the polysaccharide region from 1200 to 950 cm^{-1}, and also in the carboxylate (1450-1360 cm^{-1}) and phosphate/sulphate

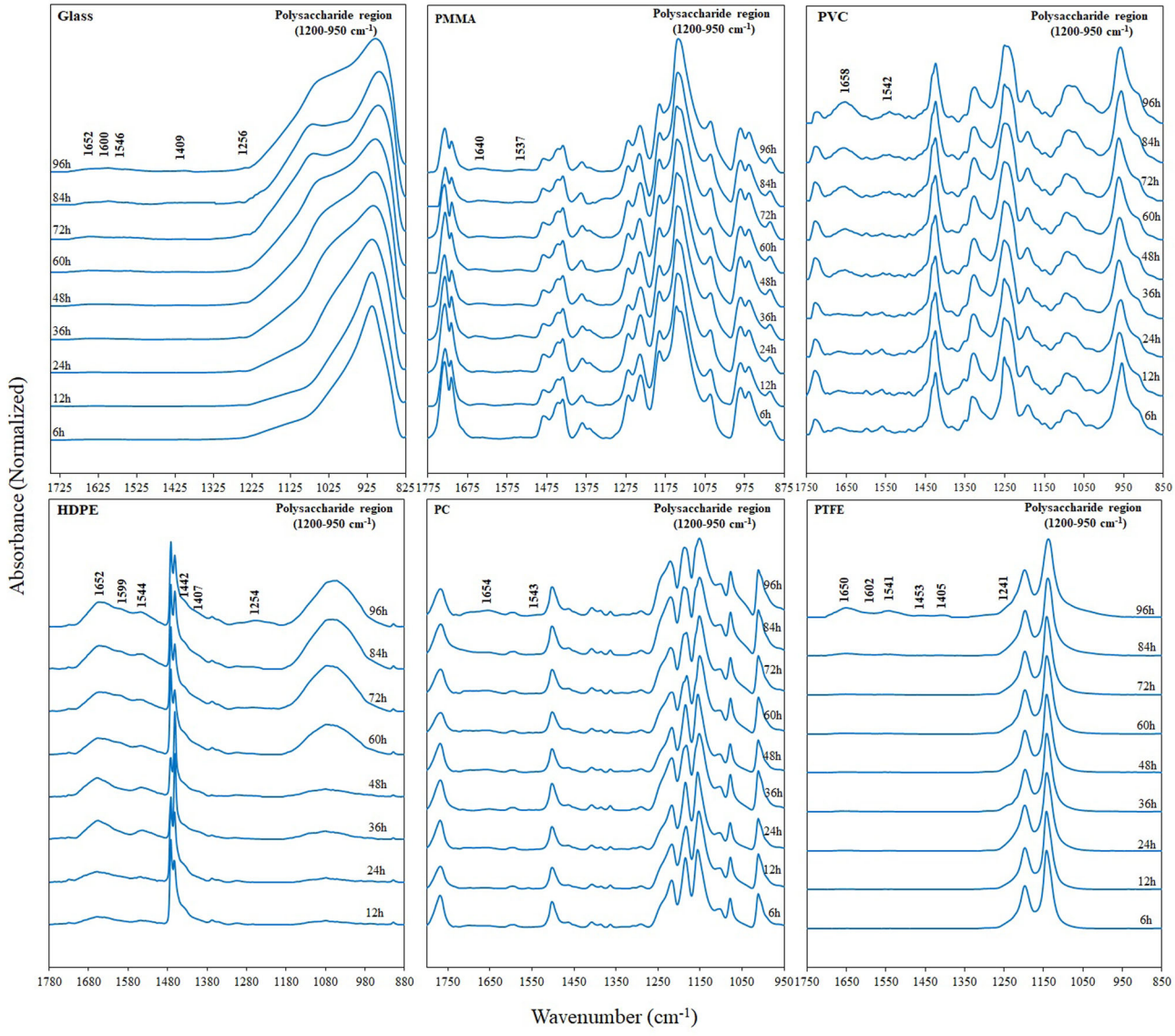

Figure 6. Time course changes in ATR-FTIR difference spectra during the initial adhesion of engineered *Anabaena* cells on different materials.

(1260-1220 cm^{-1}) regions of PMMA, PVC and PC. This is because certain substratum peaks in the spectra, including the larger substratum peaks which have absorbance > 0.8, do not subtract out completely as they may have a nonlinear absorbance/concentration relationship, and do not follow Beer's law (Smith 2011, 59–61).

The interference of these substratum peaks with the absorption peaks arising from the biomolecules makes it difficult to interpret the contributions of specific chemical functional groups within the spectra solely through spectral subtraction. Therefore, the difference spectra of all the substrata in Figure 6 were deconvoluted, and integrated peak areas were obtained in order to quantify the contribution of the important chemical functional groups/biomolecules in different regions of the spectra (Dean and Sigee 2006; Smith 2011, 72–76; Kunov-Kruse et al. 2013). The deconvoluted ATR-FTIR difference spectra of glass, PMMA, PVC, HDPE, PC and PTFE during the initial adhesion of engineered *Anabaena* at 96 h are presented together in Figure 7. The intensity (absorbance) of the substratum peaks in the ATR-FTIR spectra of all the materials was found to decrease (data not shown) with increasing time up to 96 h due to a layer of conditioning film, engineered *Anabaena* cells and EPS deposited on the materials during the adhesion process. This indicates that the interference of these substratum peaks would be much less at 96 h than at 6 h, therefore, any increase in the intensity of the peaks (integrated peak areas) in a specific region in the spectra could be attributed to the deposition of

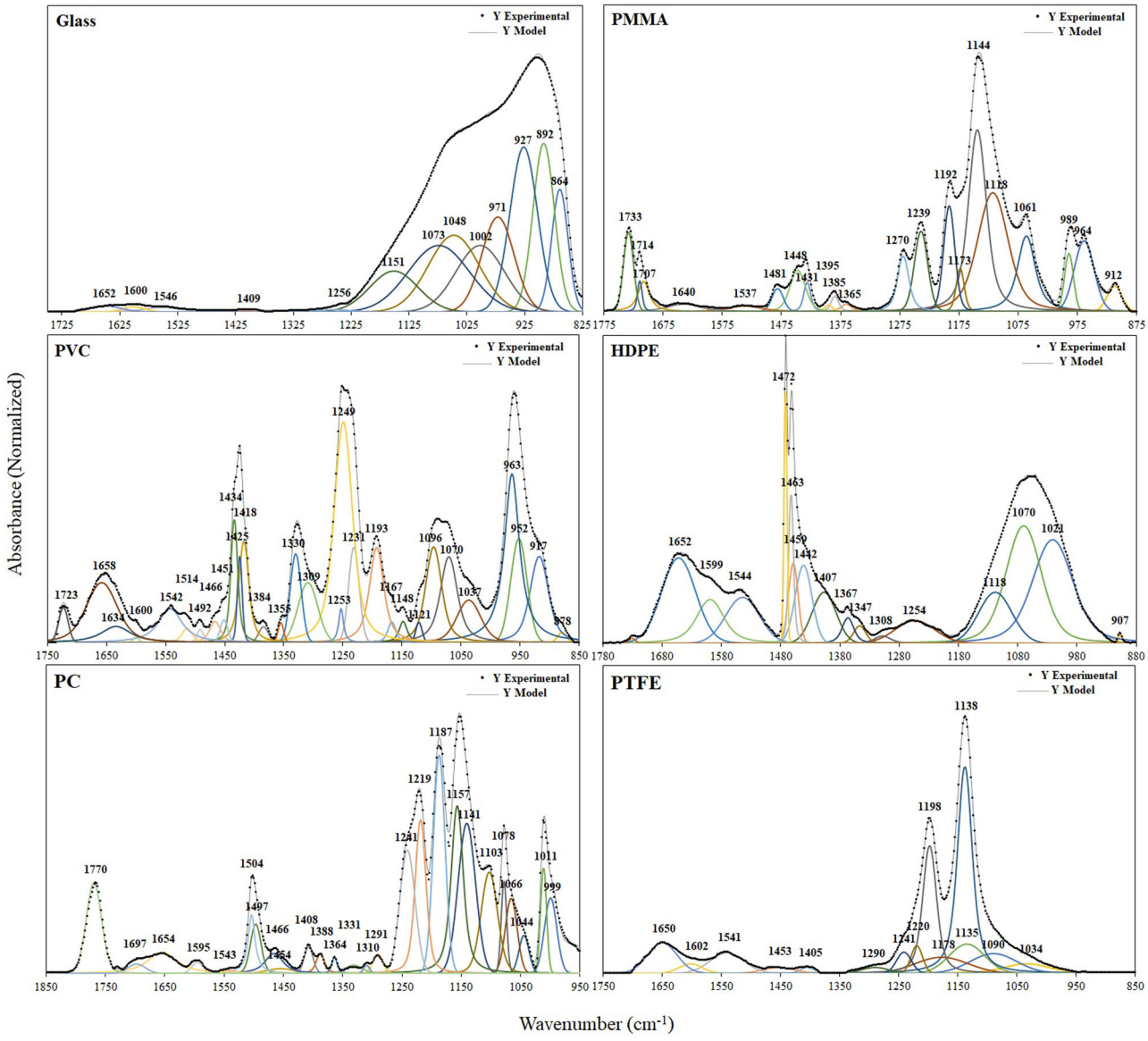

Figure 7. Deconvolution of ATR-FTIR difference spectra of materials during the initial adhesion of engineered *Anabaena* cells at 96 h.

the biomolecules related to conditioning films, and/or extracellular polymeric substances, and/or engineered *Anabaena* cells on the materials.

To a greater or lesser extent, all the substrata showed similar bands in the protein region near 1652 cm^{-1} and 1546 cm^{-1} with minor band shifts (Figure 6). The band in the region of 1652 cm^{-1} indicates C = O stretching of amide I and the band near 1546 cm^{-1} indicates N-H bending and C-N stretching of amide II (Dean and Sigee 2006). Amide I and amide II groups represent the presence of proteins on all the substrata (Dean and Sigee 2006; Ladner et al. 2010; Mota et al. 2013). According to Marcotte et al. (2007) the amide I band near 1652 cm^{-1} (C = O stretching) is sensitive to the spectral changes associated with the C-O stretching vibrations of polysaccharide (such as alginate) deposited on the materials (Marcotte et al. 2007). The band near 1600 cm^{-1} represents the C-O stretching of polysaccharides (Marcotte et al. 2007) and appears as a shoulder on the amide I band of glass, HDPE and PTFE (Figures 6 & 7). Therefore, the overlapping bands near 1652 cm^{-1} and 1600 cm^{-1} on glass, HDPE and PTFE could be an indication of polysaccharide accumulation on these surfaces (Marcotte et al. 2007).

The 1600 cm^{-1} band did not appear in the PMMA spectrum (Figures 6 and 7). In the case of PVC and PC (Figures 6 and 7), the band near 1600 cm^{-1} cannot be unambiguously assigned to C-O stretching of polysaccharides as they could be spectral interferences from the clean PVC and PC substrata. The absorption bands near 1409 cm^{-1} for glass, 1407 cm^{-1} for HDPE

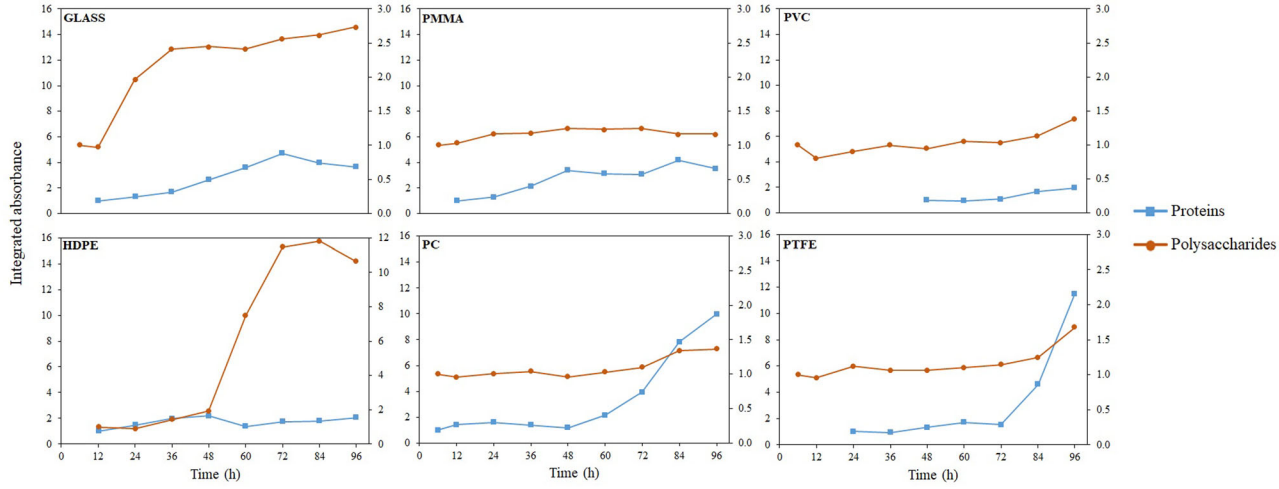

Figure 8. Fractional change in integrated peak areas of proteins (blue) (assessed from the intensity of the band near 1652 cm^{-1}) and polysaccharides (red) (assessed from the intensity of the bands between 1200-950 cm^{-1}) during the initial adhesion of engineered *Anabaena* cells on different substratum materials up to 96 h (proteins- y-axis at left; polysaccharides- y-axis at right). In the polysaccharide region, peaks that represent the wavenumbers between 1151 to 1048 cm^{-1}, 1192 to 1061 cm^{-1}, 1196 to 1037 cm^{-1}, 1118 to 1021 cm^{-1}, 1187 to 1011 cm^{-1} and 1178 to 1034 cm^{-1} on glass, PMMA, PVC, HDPE, PC and PTFE were taken for quantitative analysis. The fractional change was calculated by dividing the integrated areas of all time intervals by the integrated area of the first time interval for each substratum material.

and 1405 cm^{-1} for PTFE (Figures 6 and 7) indicate symmetric stretching of the deprotonated COO^- mode of carboxylate groups (Parikh and Chorover 2006; Lorite et al. 2011; Petrone et al. 2011). The bands near 1256 cm^{-1}, 1254 cm^{-1}, 1241 cm^{-1} which appeared for glass, HDPE and PTFE (Figures 6 and 7) arise from asymmetric stretching of SO_3^- and PO_2^- groups related to asymmetric S = O or P = O stretching vibrations of sulphate or phosphate containing compounds (Dean and Sigee 2006; Petrone et al. 2011; Mota et al. 2013).

The chemical functional groups giving rise to the wavenumber region 1200-950 cm^{-1} include contributions from both polysaccharides and symmetric stretching of PO_2^- and SO_3^- groups (Petrone et al. 2011; Petrone 2013). The broad band in the polysaccharide region on HDPE (Figures 6 and 7) indicates the presence of sulfate and phosphate group enriched polysaccharides. Phosphate stretching vibrations generally arise from the phosphodiester groups of nucleic acids (Petrone et al. 2011). Carboxylate and sulfated groups are present in most polysaccharide fractions of cyanobacteria (Di Pippo et al. 2013). These carboxylate, sulphate, phosphate groups and polysaccharides together may correspond to the presence of anionic polysaccharides (Petrone et al. 2011) secreted from engineered *Anabaena* during the settlement process.

The bands in the carboxylate (1450-1360 cm^{-1}) and phosphate/sulphate (1260-1220 cm^{-1}) regions were prominent only in the third regime (Figures 5 and 6) on glass, HDPE and PTFE which indicates that the irreversible attachment of *Anabaena* was mediated by the anionic polysaccharides on these materials. Even though the absorption intensity varied on the different materials, the existence of the amide I band near 1652 cm^{-1} on all the materials (Figures 6 and 8) in regime 1 and/or 2 suggests that proteins may be the dominant groups involved in conditioning film formation and initial adhesion of *Anabaena*.

In order to obtain quantitative information on the deposition of proteins (assessed from the intensity of band near 1652 cm^{-1}) and polysaccharides (assessed from intensity of the bands between 1200-950 cm^{-1}) during the adhesion of engineered *Anabaena* on different substrata over 96 h, the integrated peak areas of different bands obtained from deconvolution were used. Figure 8 shows the time dependent fractional change of proteins and polysaccharides, calculated by dividing the integrated areas of the protein-related or polysaccharide-related absorption bands at each time interval by the integrated areas at first time interval. The presence of proteins on all the materials was evident within 12–24 h except for PVC, which occurred at around 48 h. As there was no indication of adhesion of cells on glass, PMMA, HDPE, PC at 12 h (data not shown) or on PTFE at 24 h (Figure 3), these proteins may be attributed to the conditioning films on these substrata. On PVC, no strong cell adhesion was observed (Figure 4) at 48 h, when initial protein deposition occurred, indicating that conditioning film protein formation was delayed on PVC, compared with the other materials. The observed decrease in the

contact angles of PVC (Figure 5) within the first 12 h (Tukey's test, $p < .05$) could be due to the adsorption of conditioning film components other than proteins, as conditioning films are composed of a mixture of different molecules such as glycoproteins, humic acids, lipids, aromatic amino acids, nucleic acids, uronic acids and polysaccharides, in addition to proteins (Jain and Bhosle 2009; Thome et al. 2012). Therefore, analyzing which of these components of the conditioning films is the primary contributor to the reduction in the contact angle on PVC within 12 h might help understand the delay in protein adsorption on PVC. The fractional change in proteins between 12 to 48 h in regime 2 was higher on glass (1.6), PMMA (2.4) and HDPE (1.2) when compared to PC (0) and PTFE (0.3) (Figure 8), which could be a reason for the rapid initial adhesion of *Anabaena* cells to glass, PMMA and HDPE within 48 h (Figure 4). Between 60 and 96 h, PC (7.9) and PTFE (9.8) surfaces showed higher fractional increases in proteins than the other materials, which may correspond to the higher rate of attachment of engineered *Anabaena* cells on these surfaces in the third regime (Figure 4).

The fractional increase in polysaccharide deposition varied with respect to the different materials. A higher fractional increase in polysaccharides was observed on glass (1.5) and HDPE (0.9) between 12–48 h in regime 2. Even though rapid colonization of *Anabaena* was observed on PMMA (Figure 4), the fractional increase in polysaccharides was low (0.2) when compared with glass and HDPE between 12 and 48 h. Similarly, despite the overall higher attachment of *Anabaena* on PC and PTFE surfaces at 96 h (Figure 4), the fractional increase in polysaccharide deposition was lower (0.4 for PC and 0.6 for PTFE) than for HDPE (3.1) in the third regime. Therefore, even though extracellular polymeric substances rich in polysaccharides were reported to play a major role in bacterial adhesion to substrata, these results suggest that polysaccharide production may not be the sole mechanism responsible for different attachment behavior of engineered *Anabaena* on these materials. Altogether, the FTIR results revealed that the fractional change in the deposition of proteins on the different materials correlated reasonably well with *Anabaena* cell adhesion in regimes 2 and 3, while polysaccharide deposition was found to be surface dependent. Therefore, the nature of the different conditioning film proteins initially adsorbed in regimes 1 and 2 could be the key determinant of the extent of *Anabaena* adhesion to PBR materials. This indicates the important role of surface chemistry over material hydrophobicity and roughness in controlling *Anabaena* attachment to PBR materials.

Conclusions

Knowledge on the mechanisms of adhesion is necessary in order to prevent cyanobacterial adhesion to photobioreactor materials. Understanding the initial steps in biofilm formation such as conditioning film adsorption and its influence on the physico-chemical nature of the PBR surface is a prerequisite for gaining insights into the adhesion mechanisms of engineered *Anabaena*. Although a change in contact angles was observed within the first 6 to 12 h of the immersion of materials in an *Anabaena* suspension, conditioning film proteins were not evident on PTFE or PVC up to 24–48 h, whereas they appeared to be present on glass, PMMA, HDPE and PC within 12 h. This suggests that the time it takes for the formation of conditioning film proteins and the initial adhesion of *Anabaena* depends on the nature of the material and can be much longer for some materials (such as PVC and PTFE) than for others. Carboxylate, sulphate and phosphate group enriched polysaccharides were found to be involved in irreversible adhesion of engineered *Anabaena* on glass, HDPE and PTFE. Even though the initial colonization of *Anabaena* was relatively rapid on hydrophilic glass and PMMA (within the first 12–48 h), the rate of attachment of *Anabaena* to these substrata was relatively low in the 60–96 h period. This suggests that the engineered *Anabaena* may have had difficulty in replacing the surface bound water molecules to adhere to glass and PMMA. This confirms that hydrophilic materials such as glass and PMMA, with the ability to bind water molecules strongly through electrostatic or hydrogen bonding interactions, may be effective in creating a barrier for cell adhesion, and these materials may be worthy of further investigation as AF surfaces. The delay in protein adsorption on PVC until 48 h suggests that proteins may not be responsible for the decrease in hydrophilicity of PVC in regime 1. An in-depth understanding of the binding mechanisms of the conditioning film proteins and the negatively charged carboxylate and sulphate/phosphate groups with the different substratum materials may lead to the successful design of AF PBR materials.

Disclosure statement

No potential conflict of interest was reported by the author(s).

Funding

This work was financially supported by the National Aeronautics and Space Administration (NASA) under Grant [number NNX11AM03A], the Department of Chemical and Biological Engineering (CBE) at South Dakota School of Mines and Technology and the Composites and the Polymer Engineering (CAPE) Laboratory at South Dakota School of Mines and Technology and these organizations are greatly acknowledged by the authors.

ORCID

David R. Salem http://orcid.org/0000-0003-4216-9405

References

Auerbach ID, Sorensen C, Hansma HG, Holden PA. 2000. Physical morphology and surface properties of unsaturated *Pseudomonas putida* biofilms. J Bacteriol. 182: 3809–3815. doi:10.1128/JB.182.13.3809-3815.2000

Azeredo J, Oliveira R. 2003. The role of hydrophobicity and exopolymers in initial adhesion and biofilm formation. In: Lens P, Moran AP, Mahony T, Stoodley P, O'Flaherty V, editors. Biofilms in medicine, industry and environmental biotechnology. London (UK): IWA publishing; p. 16–31.

Beech I, Hanjagsit L, Kalaji M, Neal AL, Zinkevich V. 1999. Chemical and structural characterization of exopolymers produced by *Pseudomonas* sp. NCIMB 2021 in Continuous Culture. Microbiology. 145:1491–1497. doi: 10.1099/13500872-145-6-1491

Beech IB, Sunner JA, Hiraoka K. 2005. Microbe-surface interactions in biofouling and biocorrosion processes. Int Microbiol. 8:157–168.

Bixler GD, Bhushan B. 2012. Biofouling: lessons from nature. Proc R Soc A. 370:2381–2417. doi:10.1098/rsta.2011.0502

Brennan L, Owende P. 2010. Biofuels from microalgae—a review of technologies for production, processing, and extractions of biofuels and co-products. Renew Sust Energ Rev. 14:557–577. doi:10.1016/j.rser.2009.10.009

Callow ME, Callow JA. 2002. Marine biofouling: a sticky problem. Biologist. 49:1–5.

Callow ME, Callow JA, Ista LK, Coleman SE, Nolasco AC, López GP. 2000. Use of self-assembled monolayers of different wettabilities to study surface selection and primary adhesion processes of green algal (*Enteromorpha*) zoospores. Appl Environ Microbiol. 66:3249–3254. doi:10.1128/AEM.66.8.3249-3254.2000

Caspeta L, Buijs NA, Nielsen J. 2013. The role of biofuels in the future energy supply. Energy Environ Sci. 6: 1077–1082. doi:10.1039/c3ee24403b

Chung KK, Schumacher JF, Sampson EM, Burne RA, Antonelli PJ, Brennan AB. 2007. Impact of engineered surface microtopography on biofilm formation of *Staphylococcus aureus*. Biointerphases. 2:89–94. doi:10.1116/1.2751405

Compere C, Bellon-Fontaine MN, Bertrand P, Costa D, Marcus P, Poleunis C, Pradier CM, Rondot B, Walls M. 2001. Kinetics of conditioning layer formation on stainless steel immersed in seawater. Biofouling. 17:129–145. doi:10.1080/08927010109378472

Cui Y, Yuan WW, Pei Z. 2010. Effects of carrier material and design on microalgae attachment for biofuel manufacturing: a literature review. In: ASME 2010 International Manufacturing Science and Engineering Conference; Oct 12–15; Erie (PA): American Society of Mechanical Engineers; p. 525–540.

Cui Y, Yuan W, Cao J. 2013. Effects of surface texturing on microalgal cell attachment to solid carriers. Int J Agr Biol Eng. 6:44–54.

Damodaran VB, Murthy NS. 2016. Bio-inspired strategies for designing antifouling biomaterials. Biomater Res. 20: 18. doi:10.1186/s40824-016-0064-4

Dasgupta CN, Gilbert JJ, Lindblad P, Heidorn T, Borgvang SA, Skjanes K, Das D. 2010. Recent trends on the development of photobiological processes and photobioreactors for the improvement of hydrogen production. Int J Hydrogen Energy. 35:10218–10238. doi:10.1016/j.ijhydene.2010.06.029

De Philippis R, Sili C, Paperi R, Vincenzini M. 2001. Exopolysaccharide-producing cyanobacteria and their possible exploitation: a review. J Appl Phycol. 13: 293–299. doi:10.1023/A:1017590425924

De Philippis R, Vincenzini M. 1998. Exocellular polysaccharides from cyanobacteria and their possible applications. FEMS Microbiol Rev. 22:151–175. doi:10.1111/j.1574-6976.1998.tb00365.x

Dean AP, Sigee DC. 2006. Molecular heterogeneity in *Aphanizomenon flos-aquae* and *Anabaena flos-aquae* (Cyanophyta): a synchrotron-based Fourier-transform infrared study of lake micropopulations. Eur J Phycol. 41:201–212. doi:10.1080/09670260600645907

Di Pippo F, Ellwood NT, Gismondi A, Bruno L, Rossi F, Magni P, De Philippis R. 2013. Characterization of exopolysaccharides produced by seven biofilm-forming cyanobacterial strains for biotechnological applications. J Appl Phycol. 25:1697–1708. doi:10.1007/s10811-013-0028-1

Donlan RM. 2002. Biofilms: microbial life on surfaces. Emerg Infect Dis. 8:881–890. doi:10.3201/eid0809.020063

Dragone G, Fernandes BD, Vicente AA, Teixeira JA. 2010. Third generation biofuels from microalgae. In: Méndez-Vilas A, editor. Current Research, Technology and Education Topics in Applied Microbiology and Microbial Biotechnology. Vol. 2. Spain: Formatex Research Center; p. 1355–1366.

Ducat DC, Way JC, Silver PA. 2011. Engineering cyanobacteria to generate high-value products. Trends Biotechnol. 29:95–103. doi:10.1016/j.tibtech.2010.12.003

Duke E. 2011. Cyanofactory platform to photosynthetically produce advanced fuels and chemicals, while providing bioregenerative life support services. (NASA Proposal Number. 11-EPSCoR-0051). Rapid City: South Dakota School of Mines and Technology.

Gademann K. 2007. Cyanobacterial natural products for the inhibition of biofilm formation and biofouling. CHIMIA. 61:373–377. doi:10.2533/chimia.2007.373

Garg A, Jain A, Bhosle NB. 2009. Chemical characterization of a marine conditioning film. Int Biodeterior Biodegrad. 63:7–11. doi:10.1016/j.ibiod.2008.05.004

Genin SN, Aitchison JS, Allen DG. 2014. Design of algal film photobioreactors: material surface energy effects on algal film productivity, colonization and lipid content. Bioresour Technol. 155:136–143. doi:10.1016/j.biortech.2013.12.060

Gubner R, Beech IB. 2000. The effect of extracellular polymeric substances on the attachment of *Pseudomonas* NCIMB 2021 to AISI 304 and 316 stainless steel. Biofouling. 15:25–36. doi:10.1080/08927010009386295

Harris L, Tozzi S, Wiley P, Young C, Richardson T-M, Clark K, Trent JD. 2013. Potential impact of biofouling on the photobioreactors of the Offshore Membrane Enclosures for Growing Algae (OMEGA) system. Bioresour Technol. 144:420–428. doi:10.1016/j.biortech.2013.06.125

Hoiczyk E. 2000. Gliding motility in cyanobacteria: observations and possible explanations. Arch Microbiol. 174:11–17. doi:10.1007/s002030000187

Husmark U, Rönner U. 1993. Adhesion of *Bacillus cereus* spores to different solid surfaces: cleaned or conditioned with various food agents. Biofouling. 7:57–65. doi:10.1080/08927019309386243

Hwang G, Kang S, El-Din MG, Liu Y. 2012. Impact of conditioning films on the initial adhesion of *Burkholderia cepacia*. Colloids Surf B Biointerfaces. 91:181–188. doi:10.1016/j.colsurfb.2011.10.059

Hwang G, Liang J, Kang S, Tong M, Liu Y. 2013. The role of conditioning film formation in *Pseudomonas aeruginosa* PAO1 adhesion to inert surfaces in aquatic environments. Biochem Eng J. 76:90–98. doi:10.1016/j.bej.2013.03.024

Irving TE, Allen DG. 2011. Species and material considerations in the formation and development of microalgal biofilms. Appl Microbiol Biotechnol. 92:283–294. doi:10.1007/s00253-011-3341-0

Jain A, Bhosle NB. 2009. Biochemical composition of the marine conditioning film: implications for bacterial adhesion. Biofouling. 25:13–19. doi:10.1080/08927010802411969

Katsikogianni M, Missirlis YF. 2004. Concise review of mechanisms of bacterial adhesion to biomaterials and of techniques used in estimating bacteria-material interactions. Eur Cell Mater . 8:37–57. doi:10.22203/eCM.v008a05

Kirschner CM, Brennan AB. 2012. Bio-inspired antifouling strategies. Annu Rev Mater Res. 42:211–229. doi:10.1146/annurev-matsci-070511-155012

Kolter R, Greenberg EP. 2006. The superficial life of microbes. Nature. 441:300–302. doi:10.1038/441300a

Kunov-Kruse AJ, Riisager A, Saravanamurugan S, Berg RW, Kristensen SB, Fehrmann R. 2013. Revisiting the Brønsted acid catalysed hydrolysis kinetics of polymeric carbohydrates in ionic liquids by in situ ATR-FTIR spectroscopy. Green Chem. 15:2843–2848. doi:10.1039/c3gc41174e

Ladner DA, Jurevis JA, Clark MM. 2010. Conditioning films formed by algal biopolymers in seawater reverse osmosis desalination. Poster session presented at: The 7th IWA Leading Edge Conference on Water and Wastewater Technologies, June 2–4; Phoenix (AZ): International Water Association.

Leefmann T, Heim C, Lausmaa J, Sjövall P, Ionescu D, Reitner J, Thiel V. 2015. An imaging mass spectrometry study on the formation of conditioning films and biofilms in the subsurface (Äspö Hard Rock Laboratory, SE Sweden). Geomicrobiol J. 32:197–206. doi:10.1080/01490451.2014.910570

Lorite GS, Rodrigues CM, de Souza AA, Kranz C, Mizaikoff B, Cotta MA. 2011. The role of conditioning film formation and surface chemical changes on *Xylella fastidiosa* adhesion and biofilm evolution. J Colloid Interface Sci. 359:289–295. doi:10.1016/j.jcis.2011.03.066

Marcotte L, Kegelaer G, Sandt C, Barbeau J, Lafleur M. 2007. An alternative infrared spectroscopy assay for the quantification of polysaccharides in bacterial samples. Anal Biochem. 361:7–14. doi:10.1016/j.ab.2006.11.009

Mostafa SS, Shalaby EA, Mahmoud GI. 2012. Cultivating microalgae in domestic wastewater for biodiesel production. Not Sci Biol. 4:56–65. doi:10.15835/nsb417298

Mota R, Guimaraes R, Buttel Z, Rossi F, Colica G, Silva CJ, Santos C, Gales L, Zille A, De Philippis R, et al. 2013. Production and characterization of extracellular carbohydrate polymer from *Cyanothece* sp. CCY 0110. Carbohydr Polym. 92:1408–1415. doi:10.1016/j.carbpol.2012.10.070

Nir S, Reches M. 2016. Bio-inspired antifouling approaches: the quest towards non-toxic and non-biocidal materials. Curr Opin Biotechnol. 39:48–55. doi:10.1016/j.copbio.2015.12.012

O'Connor D. 2011. Algae as a feedstock for biofuels. An assessment of the current status and potential for algal biofuels production. Canada: S&T Consultants Inc. Available from: IEA Bioenergy's Task 39 Summary Report.

Ozkan A, Berberoglu H. 2013. Cell to substratum and cell to cell interactions of microalgae. Colloids Surf B Biointerfaces. 112:302–309. doi:10.1016/j.colsurfb.2013.08.007

Parikh SJ, Chorover J. 2006. ATR-FTIR spectroscopy reveals bond formation during bacterial adhesion to iron oxide. Langmuir. 22:8492–8500. doi:10.1021/la061359p

Parmar A, Singh NK, Pandey A, Gnansounou E, Madamwar D. 2011. Cyanobacteria and microalgae: a positive prospect for biofuels. Bioresour Technol. 102:10163–10172. doi:10.1016/j.biortech.2011.08.030

Petrone L, Easingwood R, Barker MF, McQuillan AJ. 2011. In situ ATR-IR spectroscopic and electron microscopic analyses of settlement secretions of *Undaria pinnatifida* kelp spores. J R Soc Interface. 8:410–422. doi:10.1098/rsif.2010.0316

Petrone L. 2013. Molecular surface chemistry in marine bioadhesion. Adv Colloid Interface Sci. 195-196:1–18. doi:10.1016/j.cis.2013.03.006

Quintana N, Van der Kooy F, Van de Rhee MD, Voshol GP, Verpoorte R. 2011. Renewable energy from cyanobacteria: energy production optimization by metabolic pathway engineering. Appl Microbiol Biotechnol. 91:471–490. doi:10.1007/s00253-011-3394-0

Rasband WS. 1997–2018. ImageJ. Bethesda (MD): US National Institutes of Health. https://imagej.nih.gov/ij/.

Rawat I, Kumar RR, Mutanda T, Bux F. 2013. Biodiesel from microalgae: a critical evaluation from laboratory to large scale production. Appl Energy. 103:444–467. doi:10.1016/j.apenergy.2012.10.004

Renner LD, Weibel DB. 2011. Physicochemical regulation of biofilm formation. MRS Bull. 36:347–355. doi:10.1557/mrs.2011.65

Richert L, Golubic S, Le Guédès R, Ratiskol J, Payri C, Guezennec J. 2005. Characterization of exopolysaccharides produced by cyanobacteria isolated from Polynesian microbial mats. Curr Microbiol. 51:379–384. doi:10.1007/s00284-005-0069-z

Rippka R, Deruelles J, Waterbury JB, Herdman M, Stanier RY. 1979. Generic assignments, strain histories and properties of pure cultures of cyanobacteria. Microbiology. 111:1–61. doi:10.1099/00221287-111-1-1

Ruffing AM. 2011. Engineered cyanobacteria: teaching an old bug new tricks. Bioeng Bugs. 2:136–149. doi:10.4161/bbug.2.3.15285

Schatz D, Nagar E, Sendersky E, Parnasa R, Zilberman S, Carmeli S, Mastai Y, Shimoni E, Klein E, Yeger O, et al. 2013. Self-suppression of biofilm formation in the cyanobacterium *Synechococcus elongatus*. Environ Microbiol. 15:1786–1794. doi:10.1111/1462-2920.12070

Sekar R, Venugopalan VP, Satpathy KK, Nair KVK, Rao V. 2004. Laboratory studies on adhesion of microalgae to hard substrates. In: Ang PO Jr., editors. Asian pacific phycology in the 21st century: prospects and challenges. Dordrecht (Netherlands): Springer; p. 109–116.

Siboni N, Lidor M, Kramarsky-Winter E, Kushmaro A. 2007. Conditioning film and initial biofilm formation on ceramics tiles in the marine environment. FEMS Microbiol Lett. 274:24–29. doi:10.1111/j.1574-6968.2007.00809.x

Sirmerova M, Prochazkova G, Siristova L, Kolska Z, Branyik T. 2013. Adhesion of *Chlorella vulgaris* to solid surfaces, as mediated by physicochemical interactions. J Appl Phycol. 25:1687–1695. doi:10.1007/s10811-013-0015-6

Smith BC. 2011. Fundamentals of Fourier transform infrared spectroscopy. Chapter 3, Proper use of spectral processing. 2nd ed. Boca Raton (FL): CRC Press; p. 55–85.

Thomas DJ, Sullivan SL, Price AL, Zimmerman SM. 2005. Common freshwater cyanobacteria grow in 100% CO2. Astrobiology. 5:66–74. doi:10.1089/ast.2005.5.66

Thome I, Bauer S, Vater S, Zargiel K, Finlay JA, Arpa-Sancet MP, Alles M, Callow JA, Callow ME, Swain GW, et al. 2014. Conditioning of self-assembled monolayers at two static immersion test sites along the east coast of Florida and its effect on early fouling development. Biofouling. 30:1011–1021. doi:10.1080/08927014.2014.957195

Thome I, Pettitt ME, Callow ME, Callow JA, Grunze M, Rosenhahn A. 2012. Conditioning of surfaces by macromolecules and its implication for the settlement of zoospores of the green alga *Ulva linza*. Biofouling. 28:501–510. doi:10.1080/08927014.2012.689288

Tsoglin LN, Gabel' BV, Fal'kovich TN, Semenenko VE. 1996. Closed photobioreactors for microalgal cultivation. Russ J Plant Physiol. 43:131–136.

Wang B, Lan CQ, Horsman M. 2012. Closed photobioreactors for production of microalgal biomasses. Biotechnol Adv. 30:904–912. doi:10.1016/j.biotechadv.2012.01.019

Wang D, Wu X, Long L, Yuan X, Zhang Q, Xue S, Wen S, Yan C, Wang J, Cong W. 2017. Improved antifouling properties of photobioreactors by surface grafted sulfobetaine polymers. Biofouling. 33:970–979. doi:10.1080/08927014.2017.1394457

Whitehead KA, Verran J. 2009. The effect of substratum properties on the survival of attached microorganisms on inert surfaces. In: Flemming HC, Murthy PS, Venkatesan R, Cooksey K, editors. Marine and industrial biofouling. Berlin (Germany): Springer; p. 13–33.

Yebra DM, Kiil S, Dam-Johansen K. 2004. Antifouling technology—past, present and future steps towards efficient and environmentally friendly antifouling coatings. Prog Org Coat. 50:75–104. doi:10.1016/j.porgcoat.2003.06.001

Zeriouh O, Marco-Rocamora A, Reinoso-Moreno JV, López-Rosales L, García-Camacho F, Molina-Grima E. 2019. New insights into developing antibiofouling surfaces for industrial photobioreactors. Biotechnol Bioeng. 116:2212–2222. doi:10.1002/bit.27013

Zeriouh O, Reinoso-Moreno JV, López-Rosales L, Cerón-García MC, Sánchez-Mirón A, García-Camacho F, Molina-Grima E. 2017. Biofouling in photobioreactors for marine microalgae. Crit Rev Biotechnol. 37:1006–1023. doi:10.1080/07388551.2017.1299681

Zhou R, Gibbons W. inventors; 2015. South Dakota State University, assignee. Mar 31. Genetically engineered cyanobacteria. United States patent US 8,993,303.